Journal of Applied Polymer Science

Enhanced Atomic Oxygen Erosion Resistance and Mechanical Properties of Graphene/Cellulose Acetate Composite Films

Lei Liu, Zhigang Shen, Shuaishuai Liang, Min Yi, Xiaojing Zhang, Shulin Ma
Beijing Key Laboratory for Powder Technology Research and Development, Beijing University of Aeronautics and Astronautics, 37 Xueyuan Street, Beijing 100191, People's Republic of China
Correspondence to: Z. Shen (E-mail: shenzhg@buaa.edu.cn)

ABSTRACT: The application of graphene (Gr) to enhance atomic oxygen (AO) erosion resistance and mechanical properties was demonstrated in this study. Gr-reinforced cellulose acetate (CA) composite films were obtained by flattening with a glass rod, and the AO erosion resistance was investigated in a plasma-type, ground-based AO effect simulation facility. Significant improvements in the mechanical properties and AO erosion resistance were achieved at relatively low Gr contents. A $59 \pm 7\%$ decrease in the mass loss and a $12 \pm 3\%$ increase in the tensile strength were achieved by the addition of only 1 wt % Gr. Moreover, the layered structure of the fractured surfaces and the excellent mechanical properties illustrated the homogeneous dispersion of Gr in the CA matrix and the strong interactions between Gr and CA. Furthermore, Gr flakes served as shields to defend the underside of CA from AO erosion because of the specific two-dimensional structure and outstanding AO erosion resistance. Therefore, this research provides a new and effective strategy for improving the mechanical strength and AO erosion resistance of polymer materials. © 2013 Wiley Periodicals, Inc. J. Appl. Polym. Sci. **2014**, *131*, 40292.

KEYWORDS: biodegradable; composites; films; mechanical properties

Received 15 August 2013; accepted 11 December 2013
DOI: 10.1002/app.40292

INTRODUCTION

Graphene (Gr), an exceptional two-dimensional (2D) structure material, has shown great promise in a wide variety of application areas because of its excellent electrical, thermal, and mechanical properties.[1–3] The incorporation of Gr sheets into polymers may result in significant increases in the mechanical and electrical properties.[4–9] For example, poly(vinyl alcohol)/graphene oxide composite films with only 3 wt % graphene oxide loading exhibited both a high yield strength (110 ± 7 MPa) and a high elongation at break ($36 \pm 4\%$).[10] Gr-based polymeric composites have generally been obtained with graphene oxide in most studies because graphene oxide has a low cost and can dissolve readily in most solvents.[11–14] However, there have been few reports on the mechanical strength and atomic oxygen (AO) erosion resistance of polymeric composites through the addition of Gr flakes prepared by physical exfoliation. In this study, cellulose acetate (CA), a biodegradable and natural polymer, was selected as the polymer matrix. Acetone was employed to disperse the CA and Gr flakes and could contribute to the rapid solidification of the Gr/CA composite films. Therefore, the Gr/CA composite was easily fabricated through the dispersion of Gr flakes and CA into acetone.

Spacecraft collide with ambient AO in low Earth orbit, and spacecraft materials can be oxidized and eroded by the high translational energies of AO (ca. 4–4.5 eV).[15,16] Organic polymers are widely used on spacecraft as structural and thermal protection materials because of their good chemical stability, excellent dimensional stability, and high flexural strength,[17] but organic polymers are particularly vulnerable to AO erosion. Monolayer Gr flakes have been proven to be impermeable to standard gases, and defective Gr is also suitable for impermeable membranes.[18] Therefore, the gas barrier formed by Gr flakes provides a tortuous path for the diffusion of AO and protects the underside materials from AO erosion. Moreover, AO passing through the plane of monolayer Gr needs at least 5.98 eV, and the epoxidation of Gr is the predominant chemical reaction after AO exposure. However, the minimum energy for the decomposition of epoxy groups to molecular CO is as high as 6 eV, which is higher than the energy of AO collision.[19,20] Therefore, Gr flakes can resist AO erosion and can also defend the underside of the polymer from AO erosion when Gr flakes appear on the material surface.

In this study, Gr/CA composites were prepared by the incorporation of Gr flakes into the CA matrix with acetone by fast

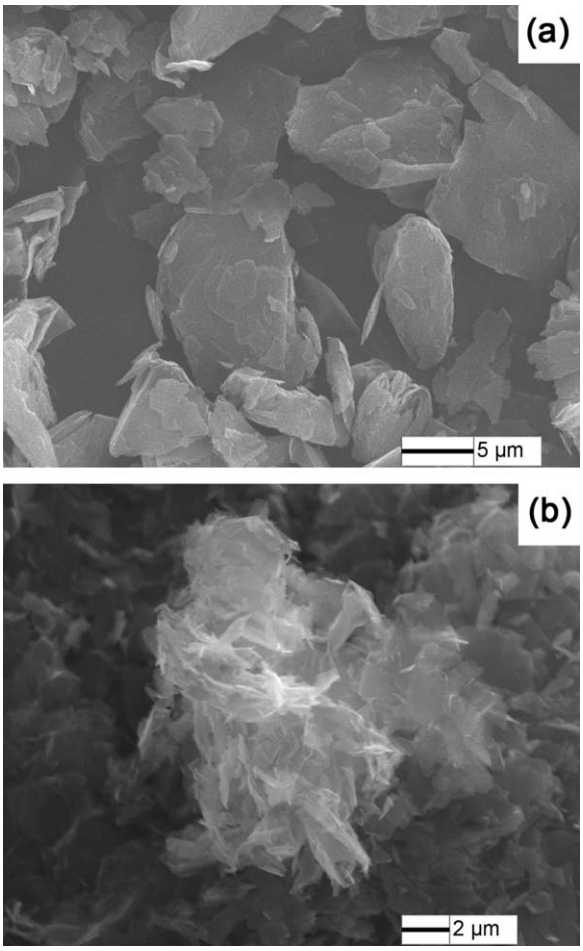

Figure 1. SEM images of the (a) graphite particles and (b) Gr flakes.

solidification processing. A significant mechanical enhancement of the Gr/CA composite films was achieved because of the unique role of Gr sheets as potential building blocks in the CA matrix. Moreover, the homogeneous dispersion and alignment of the Gr flakes increased the interfacial interaction between both components. Additionally, AO erosion resistance of the Gr/CA composites with different Gr loadings was investigated by exposure experiments in a plasma-type, ground-based AO effect simulation facility. The results clearly show that the Gr flakes formed barriers to protect the underlying CA.

EXPERIMENTAL

Preparation of the Gr/CA Composite Films

Graphite was obtained from Alfa Aesar (product number 43209). CA was purchased from Sinopharm Chemical Reagent Co., Ltd. (acetyl value = 54.5–56%). Gr flakes used as the filler were prepared by a jet cavitation method as reported previously, but the solution was changed to a mixture of 75 wt % acetone and 25 wt % deionized water.[21] The Gr dispersion was centrifuged at 500 rpm for 45 min (Beijing Jingli Centrifuge Instrument Co., Ltd., China). We obtained Gr powder by vacuum filtering the dispersions and drying them for 24 h at 60°C; it was then dispersed in acetone by sonication for 1 h to prepare the dispersion at a certain concentration (KQ2200DE, 40 kHz, Kunshan Ultrasonic Instrument Co., Ltd., China). CA (5 g) was added to the Gr dispersion (50 mL), and the mixture was subjected to magnetic stirring under sealed conditions for 4 h. The mixture was placed for 24 h to prevent air bubble entrapment. Finally, the previous solutions were flattened on the glass plate by a glass rod and were then quickly moved into a vacuum-drying oven under 32 kPa at room temperature for 1 h in a vacuum-drying method. During the coating process, the thickness of the films was easily controlled through adjustment of the height of the glass rod and the concentration of the solution. The composite films were controlled to have about 0.15, 0.25, 0.5, 0.75, and 1 wt % Gr loadings, respectively.

For comparison, the Gr/CA composite films were dried at room temperature for 2 h in an ambient drying method; we then performed the same steps as mentioned for the vacuum-drying method.

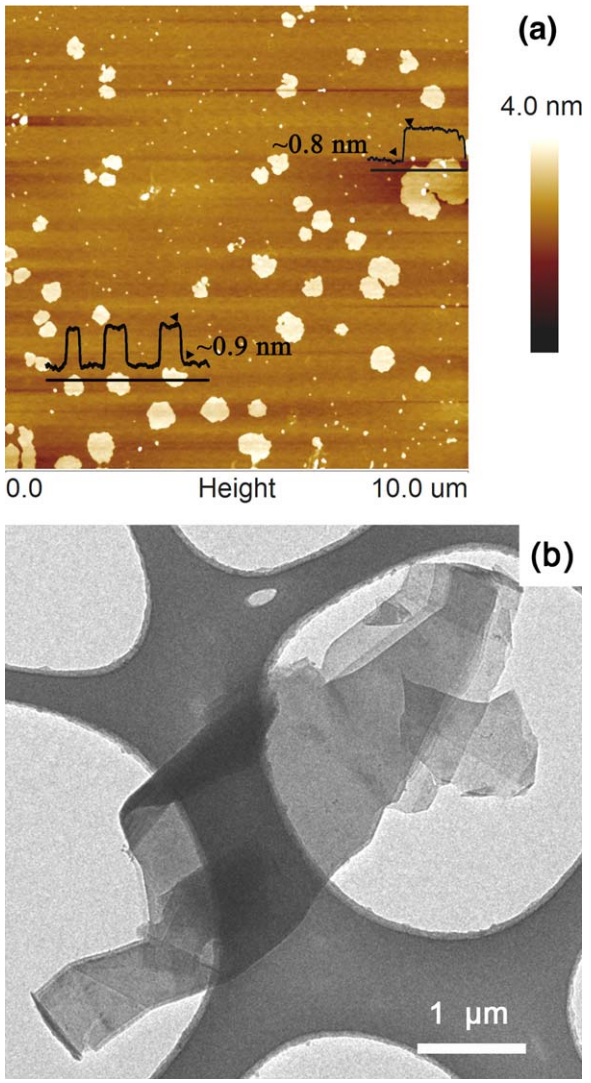

Figure 2. Representative (a) AFM and (b) TEM images of the Gr flakes. [Color figure can be viewed in the online issue, which is available at wileyonlinelibrary.com.]

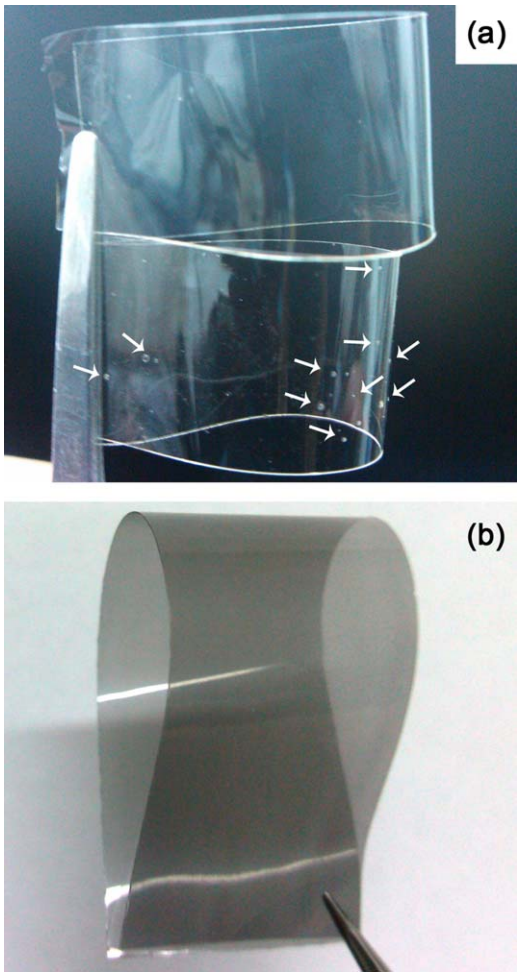

Figure 3. (a) Photograph of the pure CA film prepared by (top) vacuum drying and (bottom) ambient drying. The arrows point to bubbles. (b) Photograph of the Gr/CA composite film with 0.5% Gr loading. [Color figure can be viewed in the online issue, which is available at wileyonlinelibrary.com.]

AO Effect Simulation Experiment

The AO exposure experiment was performed in the ground-based AO effect simulation facility under 0.15 Pa; this facility was designed by our group.[22] AO was generated by the discharging of the cathode filament confined by a multiple magnetic field. After AO exposure, all of the samples were weighed, and the mass loss per unit area was calculated. In this study, the test period was about 6 h, and the AO fluence was about 1.41×10^{20} atoms/cm^2. In all cases, more than four samples were tested, from which the mean and standard deviation were calculated.

Sample Preparation and Characterization

Scanning electron microscopy (SEM) was performed on a CamScan3400 scanning electron microscope (Cambridge, England). Typical tapping-mode atomic force microscopy (AFM) measurements were performed with a multimode VIII (Bruker). Transmission electron microscopy (TEM) was done with a JEM-2100F (JEOL, Japan). We prepared the samples for AFM and TEM by dropping the Gr/acetone dispersion onto a freshly cleaved mica surface and carbon-coated copper grids (300 mesh size), respectively. The mechanical properties of the Gr/CA composites were measured by an electronic stretching machine (Instron 5565, Instron Engineering) at 19.8°C with 50% relative humidity. The extension rate was 2 mm/min. All of the samples were cut into strips 15 mm wide and 60 mm long with a razor blade. The width and thickness of each strip were measured with a low-torque digital micrometer. The reported data of the Young's modulus, tensile strength, and breaking elongation at rupture were the averages from four strips of the same sample. All of the failure occurred at the middle region of the testing strip. Thermogravimetric analysis (TGA) was performed on an STA449 instrument (Netzsch, Germany). The heating rate was 10°C/min, and approximately 15 mg of each sample was measured in an aluminum crucible under N_2.

RESULTS AND DISCUSSION

Recently, we reported the high-yield and efficient production of Gr flakes in surfactant solution by jet cavitation device (JCD), but it was difficult to remove the surfactant from the product. A mixed-solvent strategy for the preparation of Gr was proven to be green, simple, and novel.[23] Therefore, natural graphite was

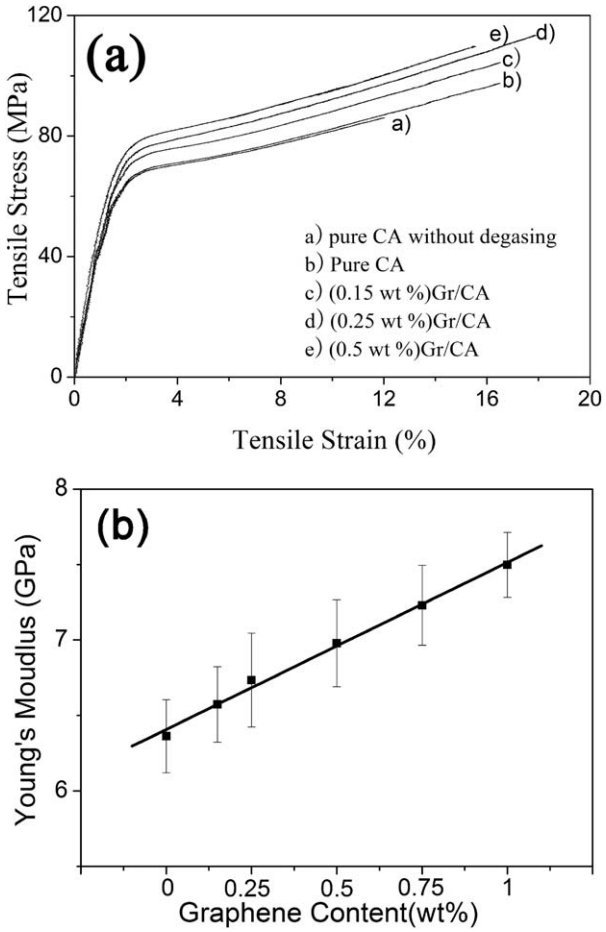

Figure 4. (a) Representative stress–strain curves of the pure CA and Gr/CA composite films with 0.15, 0.25, and 0.5 wt % Gr loadings. (b) Young's modulus and tensile strength values of the pure CA and Gr/CA composite films with 0.15, 0.25, 0.5, 0.75, and 1 wt % Gr loadings.

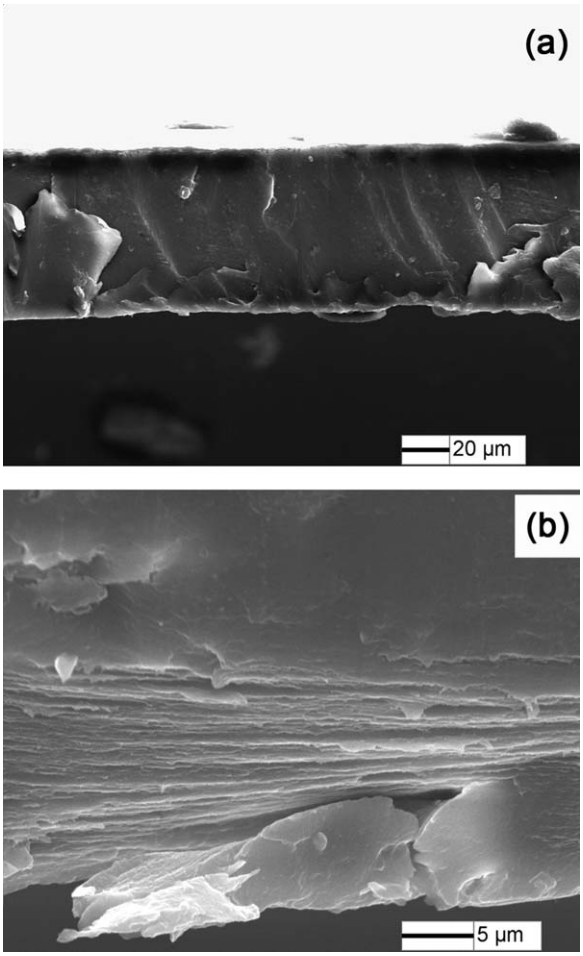

Figure 5. Fracture surfaces of the (a) pure CA film and (b) Gr/CA composite film with 0.25 wt % Gr loading after tensile testing.

dispersed in the mixture, which contained 25 wt % water and 75 wt % acetone; it was then exfoliated by a jet cavitation method in this study.[21]

The micromorphology images of natural graphite particles and Gr flakes are shown in Figure 1(a,b). There was an obvious contrast between graphite particles and Gr flakes. The size of the Gr flakes (ca. 2 μm) was smaller than that of the graphite particles (at least 5 μm). Compared with the typical layering structure of graphite particles, the Gr flakes were loose, curly, light, and transparent.

Figure 2(a) displays a typical atomic force microscopy (AFM) image of Gr flakes deposited onto a mica substrate. The height scale of the Gr flakes was about 0.8 nm; this was characteristic of fully exfoliated Gr flakes. The TEM image shows a few individual Gr flakes adhered onto each other [Figure 2(b)]. Consequently, a high-yield and stable production of Gr flakes in the water/acetone mixture by JCD was feasible.

As shown in Figure 3(a), the pure CA film without vacuum degassing had many small bubbles because of the high viscosity and surface tension of the CA solution. By comparison, bubbles were hardly found in the pure CA film, which was degassed *in vacuo*. Bubbles, which are pockets of air or solvent vapor, have adverse effects on the fracture strength and the breaking elongation of polymers. Therefore, unless otherwise mentioned, the Gr/CA composite films were prepared by vacuum degassing. The Gr/CA composite film with 0.5 wt % Gr loading was smooth, uniform, and flexible [Figure 3(b)]. The thickness of the composite films could be controlled by the height of the glass rod and the concentration of Gr flakes. Moreover, no precipitate of Gr flakes in the Gr/CA composite solution was observed after it was placed for 1 week. This indicated that the Gr flakes were steadily dispersed in CA, and the aggregation and restacking problem could be effectively avoided by the strong interfacial interactions between both components. Meanwhile, the transparency properties of the Gr/CA composite films became worse as the Gr content increased.

The typical stress–strain curves of the pure CA and Gr/CA composite films are presented in Figure 4(a). The breaking elongation of the pure CA film with vacuum degassing was higher than that of the pure CA film prepared under atmospheric conditions. This demonstrated that the reduction of the bubble defect was useful for improving the breaking elongation of the CA film, but there was no obvious improvement in Young's modulus. Compared with the those of the pure CA composite film, the tensile strength and Young's modulus of the Gr/CA composite film with 0.25 wt % Gr loading increased by 16 ± 2 and $10 \pm 2\%$, respectively. As shown in Figure 4(b), Young's modulus increased linearly with Gr content. This result was analogous to that of the poly(vinyl alcohol) film, which contained graphene oxide, and this could be explained by the shear lag model.[10,24] Gr, a 2D lattice of carbon flakes, has a significantly high surface area (2630 m^2/g).[25] Therefore, the mechanical properties of the Gr/CA composite were enhanced as a result of the Gr flakes being interlocked with CA molecules and being involved in the crosslinking of the polymer chains.[26] However, the tensile properties of the Gr/CA composite films decreased when the Gr content exceeded 0.25 wt %. These results might have been caused by the agglomeration and restacking of Gr flakes in the organic matrix and the weak interactions of chemical bonds between the inorganic and organic phases.[27] The agglomeration of Gr flakes might have been due to the specific 2D structure and high surface energy of Gr flakes; this obviously weakened the interaction between Gr and CA.

Compared with the relatively smooth fracture surface of pure CA, the fracture surface of the Gr/CA composite films with 0.25 wt % Gr loading clearly showed layered structures that were similar to those of the Gr paper and membrane (Figure 5).[28] This illustrated that the breakage of the Gr/CA composite film generally occurred in the interface between the inorganic and organic phases because the breaking strength of Gr was much higher than the attractive force of the interfaces. In addition, Gr flakes tended to align parallel to the film surface on account of the surface tension of the composite solution, the particular 2D structure of Gr, and gravitational forces.[29] The homogeneous dispersion of Gr flakes in CA improved the stress transfer and enhanced the adhesion between the Gr flakes and CA. Therefore, the Gr/CA composite films combined the ductile properties of the polymer and the excellent breaking strength of Gr.

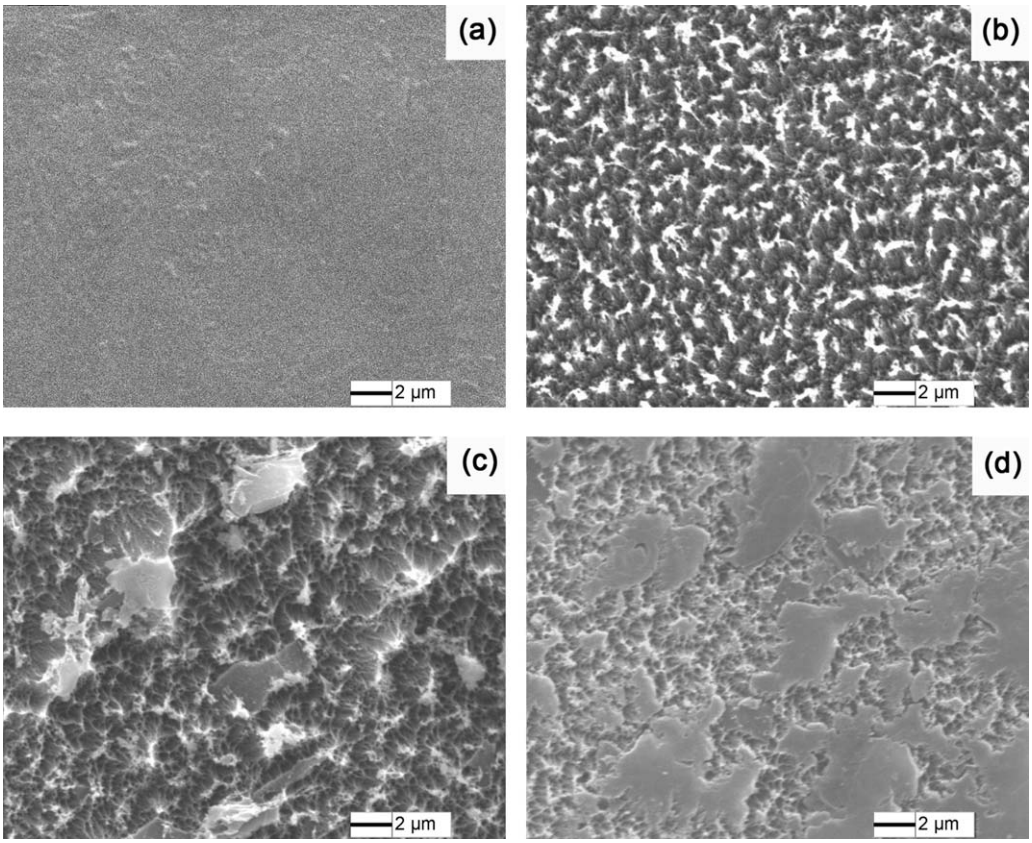

Figure 6. SEM images of the pure CA film (a) before and (b) after AO exposure and the Gr/CA composite film with (c) 0.25 and (d) 1 wt % Gr loadings after AO exposure.

As shown in Figure 6(a), the surface of the pure CA sample was relatively smooth before AO exposure. However, Figure 6(b) shows that the pure CA became significantly roughened and formed a homogeneous deep-valley peak risk microstructure after AO exposure. This demonstrated that the pure CA was significantly eroded by AO. The translational energy of AO collisions was about 4.5–5 eV; this was sufficient to break the polymer bond and induce oxidative decomposition.[15,16] Figure 6(c) shows the surface morphology of the Gr/CA composite containing 0.25 wt % Gr. Comparing Figure 6(b) with Figure 6(c), one can see that the surface characteristics of the Gr/CA composite sample were significantly different from those of the pure CA sample after AO exposure. The CA on the surface was eroded in the early stages, and Gr flakes were exposed on the surface of the Gr/CA composite after AO exposure. Compared with the surface of the Gr/CA composite with 0.25 wt % Gr loading, more Gr flakes covered the underlying CA to prevent

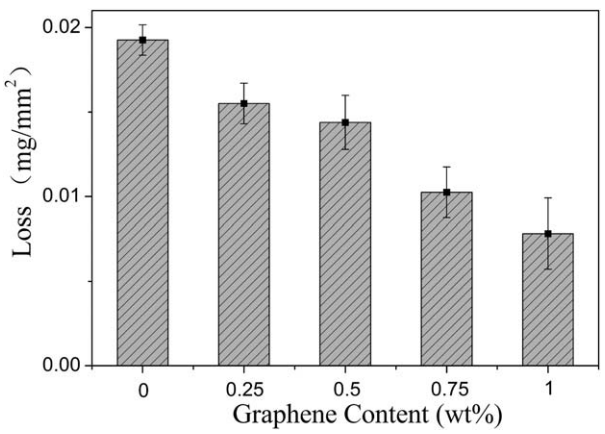

Figure 7. Mass loss of the pure CA and Gr/CA composites with 0.25, 0.5, 0.75, and 1 wt % Gr loadings.

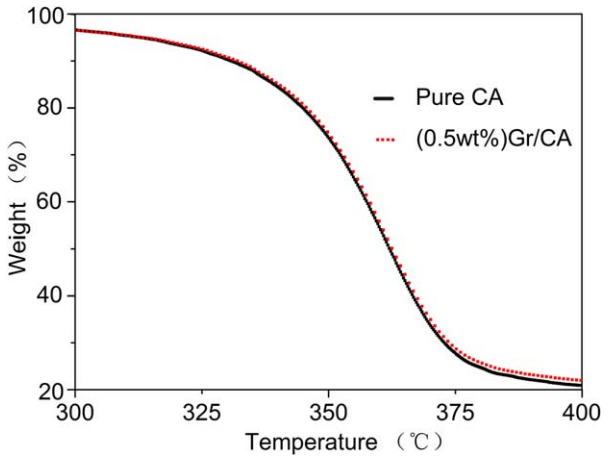

Figure 8. TGA curves of the pure CA film and Gr/CA composite film containing 0.5 wt % Gr. [Color figure can be viewed in the online issue, which is available at wileyonlinelibrary.com.]

CA from further AO erosion in the surface of the Gr/CA composite with 1 wt % Gr loading [Figure 6(d)].

Figure 7 shows that the mass loss of the Gr/CA composites decreased with increasing Gr content. Compared with pure CA, the mass loss of the Gr/CA composite film with 1 wt % Gr decreased by 59 ± 7%. As shown in Figure 6, the larger the filling amount of Gr was, the more Gr covered the surface after AO erosion. Consequently, this illustrated that the AO erosion resistance of CA improved with Gr flake filler. Gr has a special and stable 2D structure and has a high surface area;[24] this contributed to the enlargement of the coverage area on the surface after AO exposure. In addition, the layered structures formed by Gr flakes, which are very impermeable to gas atoms, were effective in preventing AO from passing through, so the Gr flakes also enhanced the gas barrier properties of the Gr/CA composite. Exceptionally, the Gr structure was stable under AO exposure because the oxidative decomposition energy of Gr was higher than the AO energy.[30] More Gr exposed on the surface better protected the underside of CA from AO erosion. All of these results indicate that the horizontal layered structure, which was formed by the uniform dispersion of Gr, successfully protected the underside of CA from AO erosion.

TGA was further used to determine the thermal properties of the pure CA film and Gr/CA composite film with 0.5 wt % Gr (Figure 8). The decomposition process of the Gr/CA composite films was similar to that of the pure CA film, and the peak degradation temperature of the Gr/CA composites with 0.5 wt % Gr loading (obtained from the derivative of the TGA curves) was about 2.8°C higher than that of pure CA. These results indicate that the Gr flakes improved the thermal stability of CA because of the mobility of the polymer segments at the interfaces of CA and Gr flakes was suppressed by strong interactions.

CONCLUSIONS

We have reported a simple approach for fabricating excellent mechanical properties and significant AO-erosion-resistance materials based on CA. The layered structures' fracture surface and excellent improvement in mechanical properties illustrated that the Gr flakes were homogeneously dispersed in the CA. Compared with the pure CA, evident improvements in the tensile strength and AO erosion resistance of the Gr/CA composites were achieved by the addition of a few Gr flakes. It should be emphasized that the 2D Gr flakes could prevent AO erosion and protect the material underneath. For this reason, Gr could be further applied to the enhancement of the AO erosion resistance of spacecraft material and to obtain excellent comprehensive performance.

ACKNOWLEDGMENTS

This work was funded by Beijing Natural Science Foundation (contract grant number 2132025), the Special Funds for the Co-Construction Project of Beijing Municipal Commission of Education, and the Fundamental Research Funds for the Central Universities, the Innovation Foundation of Beijing University of Aeronautics and Astronautics for Ph.D. Graduates, and the Innovative Practice Foundation of Beijing University of Aeronautics and Astronautics for Graduates (contract grant number YCSJ01201309). The Specialized Research Fund for the Doctoral Program of Higher Education (contract grant number 20131102110016).

REFERENCES

1. Novoselov, K.; Geim, A. K.; Morozov, S.; Jiang, D.; Zhang, Y.; Dubonos, S.; Grigorieva, I.; Firsov, A. *Science* **2004**, *306*, 666.
2. Novoselov, K.; Geim, A. K.; Morozov, S.; Jiang, D.; Grigorieva, M. K. I.; Dubonos, S.; Firsov, A. *Nature* **2005**, *438*, 197.
3. Leenaerts, O.; Partoens, B.; Peeters, F. *Appl. Phys. Lett.* **2008**, *93*, 193107.
4. Kim, H.; Abdala, A. A.; Macosko, C. W. *Macromolecules* **2010**, *43*, 6515.
5. Su, Q.; Pang, S.; Alijani, V.; Li, C.; Feng, X.; Müllen, K. *Adv. Mater.* **2009**, *21*, 3191.
6. Eda, G.; Chhowalla, M. *Nano Lett.* **2009**, *9*, 814.
7. Li, M.; Jeong, Y. G. *J. Appl. Polym. Sci.* **2012**, *125*, 532.
8. Lim, Y. S.; Tan, Y. P.; Lim, H. N.; Tan, W. T.; Mahnaz, M. A.; Talib, Z. A.; Huang, N. M.; Kassim, A.; Yarmo, M. A. *J. Appl. Polym. Sci.* **2013**, *128*, 224.
9. Polschikov, S. V.; Nedorezova, P. M.; Klyamkina, A. N.; Kovalchuk, A. A.; Aladyshev, A. M.; Shchegolikhin, A. N.; Shevchenko, V. G.; Muradyan, V. E. *J. Appl. Polym. Sci.* **2013**, *127*, 904.
10. Xu, Y.; Hong, W.; Bai, H.; Li, C.; Shi, G. *Carbon* **2009**, *47*, 3538.
11. Cao, Z.; Song, P.; Fang, Z.; Xu, Y.; Zhang, Y.; Guo, Z. *J. Appl. Polym. Sci.* **2012**, *126*, 1546.
12. Fim, F. D. C.; Basso, N. R. S.; Graebin, A. P.; Azambuja, D. S.; Galland, G. B. *J. Appl. Polym. Sci.* **2013**, *128*, 2630.
13. Kranbuehl, D. E.; Cai, M.; Glover, A. J.; Schniepp, H. C. *J. Appl. Polym. Sci.* **2011**, *122*, 3739.
14. Ma, F.; Yuan, N.; Ding, J. *J. Appl. Polym. Sci.* **2013**, *128*, 3870.
15. Su, L.; Tao, L.; Wang, T.; Wang, Q. *Polym. Degrad. Stab.* **2012**, *97*, 981.
16. Xiao, F.; Wang, K.; Zhan, M. S. *J. Mater. Sci.* **2012**, *47*, 4904.
17. Reddy, M. R. *J. Mater. Sci.* **1995**, *30*, 281.
18. Bunch, J. S.; Verbridge, S. S.; Alden, J. S.; van der Zande, A. M.; Parpia, J. M.; Craighead, H. G.; McEuen, P. L. *Nano Lett.* **2008**, *8*, 2458.
19. Vinogradov, N.; Schulte, K.; Ng, M. L.; Mikkelsen, A.; Lundgren, E.; Martensson, N.; Preobrajenski, A. *J. Phys. Chem. C* **2011**, *115*, 9568.
20. Sun, T.; Fabris, S. *Nano Lett.* **2011**, *12*, 17.
21. Shen, Z.; Li, J.; Yi, M. *Nanotechnology* **2011**, *22*, 365306.
22. Zhao, X.-H.; Shen, Z.-G.; Xing, Y.-S.; Ma, S.-L. *Polym. Degrad. Stab.* **2005**, *88*, 275.
23. Yi, M.; Shen, Z.; Ma, S.; Zhang, X. *J. Nanopart. Res.* **2012**, *14*, 1.
24. Bonderer, L. J.; Studart, A. R.; Gauckler, L. *J. Science* **2008**, *319*, 1069.

25. McAllister, M. J.; Li, J.-L.; Adamson, D. H.; Schniepp, H. C.; Abdala, A. A.; Liu, J.; Herrera-Alonso, M.; Milius, D. L.; Car, R.; Prud'homme, R. K. *Chem. Mater.* **2007**, *19*, 4396.

26. Liang, J.; Huang, Y.; Zhang, L.; Wang, Y.; Ma, Y.; Guo, T.; Chen, Y. *Adv. Funct. Mater.* **2009**, *19*, 2297.

27. Podsiadlo, P.; Kaushik, A. K.; Arruda, E. M.; Waas, A. M.; Shim, B. S.; Xu, J.; Nandivada, H.; Pumplin, B. G.; Lahann, J. *Science* **2007**, *318*, 80.

28. Chen, C.; Yang, Q. H.; Yang, Y.; Lv, W.; Wen, Y.; Hou, P. X.; Wang, M.; Cheng, H. M. *Adv. Mater.* **2009**, *21*, 3007.

29. Dikin, D. A.; Stankovich, S.; Zimney, E. J.; Piner, R. D.; Dommett, G. H.; Evmenenko, G.; Nguyen, S. T.; Ruoff, R. S. *Nature* **2007**, *448*, 457.

30. Topsakal, M.; Şahin, H.; Ciraci, S. *Phys. Rev. B* **2012**, *85*, 155445.